

Nozzle Displacement Effects on Two-Phase Ejector Performance: An Experimental Study

K. Ameer[†] and Z. Aidoun

Canmet ENERGY, Natural Resources Canada, Varennes, Qc, J3X1S6, Canada

[†]Corresponding Author Email: khaled.ameur@canada.ca

(Received September 8, 2017; accepted January 13, 2018)

ABSTRACT

Experimental results of two-phase ejector operation with refrigerant R134a as working fluid are presented in this paper. The tests carried out allowed evaluating the influence of the primary nozzle position in the mixing chamber and of operating conditions such as the thermodynamic state of the fluid at the inlet and outlet of the ejector. Various positions of the primary nozzle were tested and the operating conditions ranges were: primary inlet pressure 8.8-14.9 bars, subcooling 0.2-5 °C and ejector outlet pressure 3.7-4.7 bars. The tests have shown an optimal position of the primary nozzle (NXP=38.1 mm) in the ejector but this position was not very sensitive to operational conditions. The performance of the ejector dropped sharply when the nozzle was placed right at the inlet of the constant-area section in the mixing chamber. Pressures at the primary inlet and outlet had a limited impact on the entrainment ratio (<10%), but it was found that the level of subcooling at the inlet of the primary flow had an important influence on the entrainment ratio with a variations of about 66%. Pressure monitoring inside the ejector showed a strong relation between NXP and pressure variations in the mixing section and the diffuser.

Keywords: Experiments; Two-phase; Ejector; R134a; NXP.

NOMENCLATURE

D diameter, mm
L length, mm
mass flow rate, kg/s
P pressure, Pa
T temperature, °C

Greeks

Δ difference
 ΔT_{sub} subcooled temperature, °C
 τ compression ratio
 φ entrainment ratio
 ω entrainment ratio

Subscripts

conv convergent

div divergent
in inlet
prim primary
sec secondary
sat saturated
sub subcooling
out outlet
t throat

Acronym

COP Coefficient of Performance
NXP Nozzle Exit Position
RTD Resistance Temperature Detector

1. INTRODUCTION

In the context of increasing global energy demand and growing environmental concerns, ejectors can be considered as a simple and effective way to address these issues. Indeed, ejectors are increasingly used in industrial processes and refrigeration systems to improve performance and energy efficiency (Chen, 2015).

Ejector (see Fig. 1) is a static device with no moving parts. A high-pressure stream (primary flow) expands through the primary nozzle. As a result, a low-pressure zone is created in the suction

chamber in such a way that a lower energy flow (secondary flow) is drawn through the secondary inlet. Primary and secondary flows mix inside the mixing chamber, and the shock interactions between streams results in a first pressure increase. The flow resulting from this phase is further compressed in the diffuser.

However, despite their simple geometry, their design remains complex as geometric parameters and working conditions can have significant impact on their overall operation.

Geometrical factors and operational conditions have been the subject of many experimental and

numerical studies, especially single phase ejectors. However, those related to two-phase ejectors are still limited.

Among geometrical factors, the position of the primary nozzle with respect to the mixing chamber may strongly influence the performance of the ejector. The nozzle exit position (NXP) is generally defined as the relative distance of the primary nozzle outlet to the mixing chamber inlet (Fig. 1). NXP value is positive downstream and negative upstream of the mixing chamber entrance, respectively.

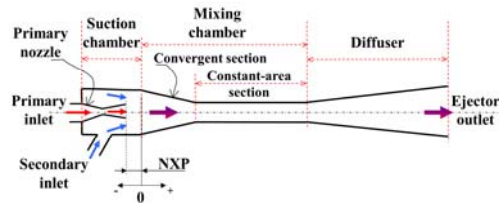


Fig. 1. Main parts of the ejector and the nozzle position (NXP).

Aphornratana and Eames (1997) tested a movable nozzle in a steam ejector of a 2 kW refrigerator. By moving the primary nozzle to the mixing chamber, the evaporator temperature decreased to a minimum and then increased. The authors considered that the minimum temperature reached matched the optimal position, since it corresponded to the highest compression ratio. The optimal NXP obtained was in the range of 0 to 15 mm. However, this nozzle position depended on the pressure of both primary inlet and ejector outlet. Chunnanond and Aphornratana (2004) by moving the nozzle of a steam ejector towards the mixing chamber, observed a decrease in the COP due to the cooling capacity reduction and an increase of the critical pressure. Measurement of the pressure inside the ejector allowed the authors to speculate on its trend. By removing the nozzle from the mixing chamber, a large converging duct cross section (space between the ejector wall and the primary jet) could be made available due to the decrease in the expansion angle of the primary jet. Thus, the cooling capacity and the COP were improved since more secondary fluid was drawn. The decrease of the critical pressure that accompanies this phenomenon was explained by the choking position moving upstream. This was due to the reduction of momentum in the mixed flow drawing more of the secondary stream. With R245fa as refrigerant, Eames *et al.* (2007) were able to show the strong influence of NXP on the ejector entrainment ratio and globally on the performance of the refrigeration system. In some cases the COP varied by 40%. The optimal NXP was obtained by positioning the nozzle at 5 mm upstream of the mixing chamber.

Hu *et al.* (2014) experimented a two-phase ejector with the refrigerant R410A, in an air conditioning system. The distance between the nozzle outlet and the constant section mixing chamber was varied from 0 to 9 mm. An optimal position of the nozzle for system capacity and performance was found to be 3mm. Experimental results obtained by Wang

and Yu (2016) with an R600a two-phase ejector showed no optimal position. An increase of entrainment ratio with NXP was observed, but at 6 mm upstream of the mixing chamber, the entrainment ratio tended to remain constant. Ameur *et al.* (2016, 2017) performed several experimental tests on a two-phase ejector test bench with refrigerant R134a under various subcooling degrees and close to saturation. The critical conditions of the primary flow were analysed with no secondary flow suction. The obtained results showed that the critical mass flow rate increased with the primary pressure and the level of subcooling. The necessary expansion to reach the critical conditions was not very sensitive to the pressure imposed on the primary flow stream, but it increased substantially with the degree of subcooling. Liu *et al.* (2012) investigated the effects of various ejector geometries and operating conditions on the performance of an air conditioner working with CO₂ under trans-critical conditions. A maximum COP value was reached when the motive nozzle exit positioned before the mixing chamber inlet was three times the diameter of the constant-area mixing section.

Modelling NXP effects with a thermodynamic approach is rather intricate and CFD numerical techniques are more appropriate for such a task. CFD modeling of two-phase flow process inside the ejector is not an easy task (Yazdani *et al.*, 2012), and currently this approach is increasingly used for single-phase ejectors. Zhu *et al.* (2009) investigated nozzle displacement in a single-phase ejector with R141b. The entrainment ratio was improved by retracting the nozzle from the mixing chamber in the range of 12 to 30 mm. The authors have also shown that the NXP depended on the diameter of the mixing chamber, as well as of the pressure at the primary inlet. The impact of NXP on the critical pressure and entrainment ratio for a steam ejector experimentally found by Chunnanond and Aphornratana (2004) was later confirmed by Varga *et al.* (2009) by means of a CFD based analysis. The optimal position of the nozzle was found to be located at 60 mm inside the mixing chamber, for an improvement in the entrainment ratio of 5%-12%. Lin *et al.* (2013) also used CFD to investigate geometry parameters of an adjustable ejector with the refrigerant R134a. For the case with no spindle, the pressure recovery of the ejector slightly increases until a NXP of -2.5 mm, and then decreases as the NXP increases. A very slight displacement of this peak position was observed with the use of the spindle to adjust the throat area.

Banasiak *et al.* (2014) developed a CFD analysis of a two-phase CO₂ trans-critical ejector. The authors first performed an exergy analysis, identifying the mixing chamber zone as a significant source of irreversibility, then they numerically examined the influence of the mixing chamber diameter and length on the overall ejector performance was. More recently, Palacz *et al.* (2017) investigated the geometry optimisation of a two-phase CO₂ trans-critical ejector. Six geometrical parameters were considered: three of them are related to the mixing

section and the remaining parameters to the motive nozzle. Results showed that the suction nozzle shape had less significant influence on the ejector performance than motive nozzle and mixing chamber geometries.

In recent years a new type of primary nozzle with two throats was proposed. The primary nozzle is a combination of two convergent-divergent in series. The expanded refrigerant liquid into this nozzle generates very small drops and reaches sonic conditions at the second throat. Ren *et al.* (2014) tested this nozzle in a two-phase ejector refrigeration cycle with R134a. The authors showed that the entrainment ratio could be improved by 18% and the COP of the system by 12% compared to using an ejector with one throat. The concept of the two-throat nozzle was also tested with transcritical CO₂ (Huai *et al.*, 2017) in a refrigeration system. The experiment showed an increase of COP by up to 32.4% relative to the conventional system without ejector

In the present paper, experiments were performed on a two-phase ejector using R134a as operating refrigerant. The main objective of this study was to analyse in detail the influence of the NXP value on the ejector performance. Working conditions in a range of stable operation were tested. In addition, pressure probes strategically located inside the mixing chamber made it possible to monitor the impact of the NXP variation on the pressure distribution profile inside the ejector.

2. EXPERIMENTAL SETUP

Figure 2 shows the experimental test facility available at CanmetENERGY laboratory and used to generate results for the present paper. The test bench was designed to offer flexibility for parameters variation in a wide range of conditions. A simplified diagram of the main loop working with the refrigerant R134a and integrating the ejector is shown in Fig. 3. Four auxiliary loops reproducing heat and source sinks are connected to the principal loop through brazed plate type heat exchangers. All loops are fed by propylene-glycol and water cooling fluids according to temperature levels required for the process. A combination of R507 refrigeration unit and a set of electrical heating are used to maintain these loops at the required temperature levels.

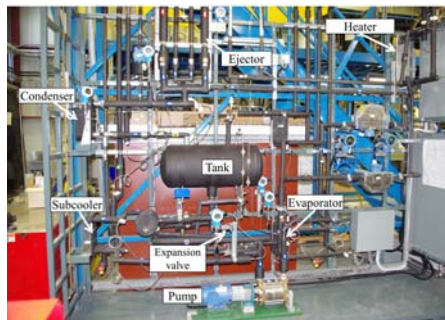


Fig. 2. Experimental two-phase ejector test facility.

A pump feeds high pressure liquid refrigerant to the ejector primary inlet. The pressure of this primary stream is controlled by varying the speed of the pump; the inlet temperature and the level of subcooling are imposed on the fluid by modulating the heating power.

Referring to Fig. 1 above the primary liquid stream expands in the nozzle, creating partial but sufficient vacuum to draw some amount of vapour from the secondary inlet into the mixing chamber. At the outlet of the ejector, the two-phase mixture is all fed to a condensing unit and the condensate is recovered in a reservoir. Part of this liquid is circulated through a subcooler and then to the pump. The remaining liquid undergoes an isenthalpic expansion by means of an electric valve to feed the evaporator. The pressure at the secondary inlet is controlled by adjusting the electric valve. Secondary flow superheating depends on the heat supplied to the evaporator. The discharge pressure at the diffuser exit is controlled by the temperature and the flow rate of the propylene-glycol entering the condenser.

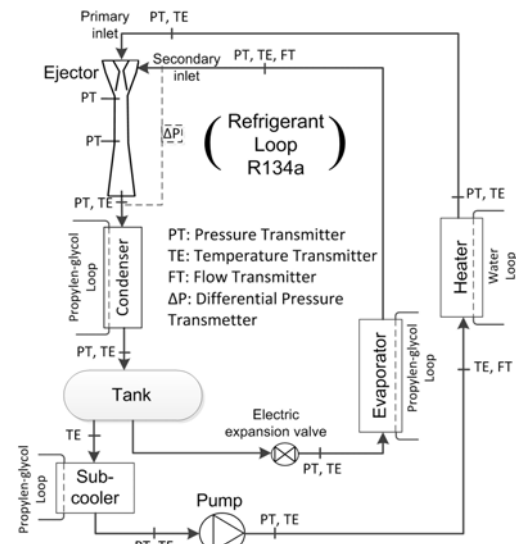


Fig. 3. Diagram of the test rig.

The test rig is well equipped with high quality instrumentation, more particularly the ejector loop. The main parameters measured, include temperatures, pressures, flow rates for vapour and liquid phases. Primary and secondary mass flow rates are measured by Coriolis flow meters, located downstream of the heater and evaporator respectively. The accuracy of the flow measurement is within 0.75% and 0.3% of the full scale for respectively vapour and liquid refrigerant. Water and propylene-glycol flow rates are measured by magnetic flow meters with an error of 0.5%. The temperatures are measured by RTD sensors having an accuracy of ± 0.05 °C. Pressure is measured with metallic membrane transducers within 0.075% of the set span.

The ejector is equipped with a system that allows an easy displacement of the primary nozzle within the mixing chamber. The main geometry

specifications of the ejector are summarized in table 1 below.

Table 1 Ejector dimensions

		Diameter (mm)	Length (mm)	Angle (°)
Primary Nozzle	CS	$D_{in}=10$ $D_r=1.39$ $D_{out}=4.09$	$L_{conv}=9.7$ $L_{div}=38$	$\phi_{conv}=45$ $\phi_{div}=4$
	CAS	$D_{in}=44.9$ $D_{out}=6.9$	45.7	45
Mixing chamber	CS	$D_{in}=6.9$ $D_{out}=31.8$	134.26	11
	CAS	6.9	164.3	-
Diffuser		$D_{in}=6.9$ $D_{out}=31.8$	134.26	11

CS: convergent section, CAS: constant-area section

3. RESULTS AND DISCUSSION

The experimental results presented in this paper are mainly focused on the two-phase ejector performance for various positions of the primary nozzle inside the mixing chamber. Operational conditions at the ejector inlets and outlet were also varied.

The primary nozzle position was tested in the range of NXP=-10 mm to 44.4 mm. Pressure at the primary inlet was varied from 8.8 to 14.9 bar and the pressure at the ejector outlet from 3.7 to 4.7 bar. The pressure at the secondary inlet adapted to the reigning conditions, on the other hand a degree of superheat of around 10 °C was maintained at this inlet. During the tests, the expansion valve before the evaporator was kept almost completely open, which resulted in a secondary pressure slightly lower than the outlet ejector pressure.

Three levels of subcooling at the ejector primary inlet were tested (0.2 °C, 1 °C, 5 °C). Subcooling is evaluated by Eq. (1) below, based on the temperature and the pressure measurements at the primary fluid inlet.

$$\Delta T_{sub} = T_{sat}(P_{prim}) - T_{prim} \quad (1)$$

The ejector performance is mainly represented by two parameters: the entrainment ratio ω (Eq. (2)) and the compression ratio τ (Eq. (3)).

$$\omega = \frac{\dot{m}_{sec}}{\dot{m}_{prim}} \quad (2)$$

$$\tau = \frac{P_{out}}{P_{sec}} \quad (3)$$

(Fig. 5b) is low. A maximum variation of about 2% is observed at the nozzle optimal position.

3.1. Primary Inlet Subcooling and NXP

Figure 7 displays the effects of the primary subcooling on the performance of the ejector, for various positions of the primary nozzle. The entrainment ratio, primary-secondary mass flow rates and the compression ratio are reported for three subcooling levels: 0.2 °C, 1 °C and 5 °C. Pressures at the primary inlet and at the ejector

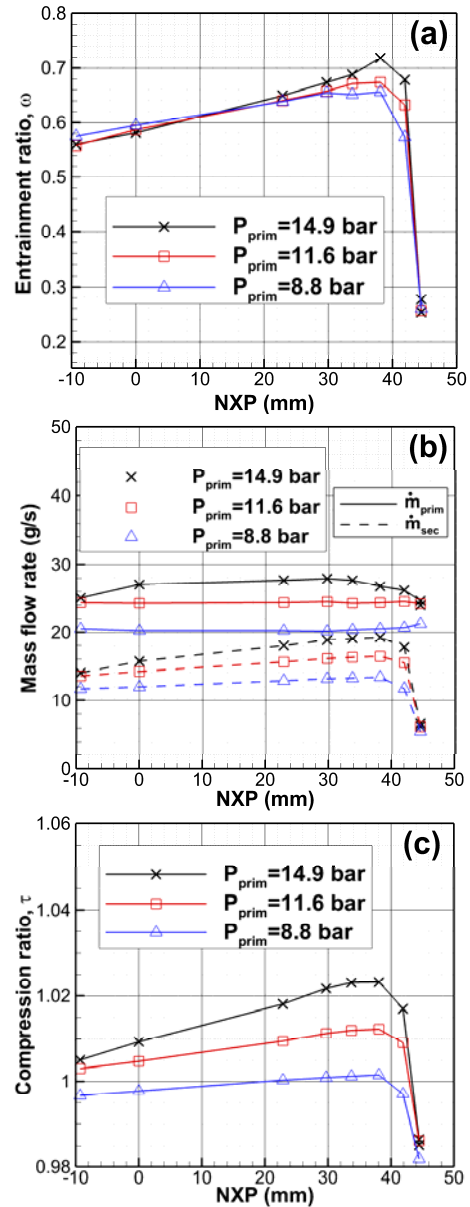


Fig. 5. Primary inlet pressure and NXP: (a) entrainment ratio (b) mass flow rate (c) compression ratio.

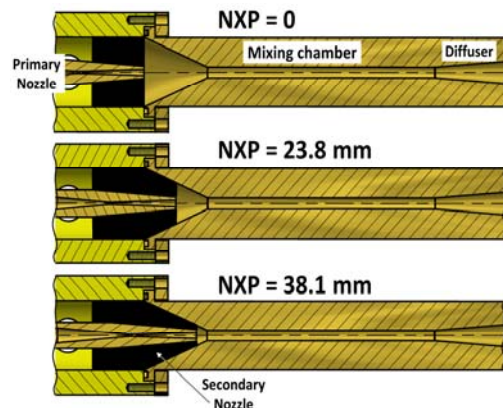


Fig. 6. Variation of the secondary nozzle shape with NXP.

outlet are maintained constant respectively at

14.9 bar and 3.7 bar.

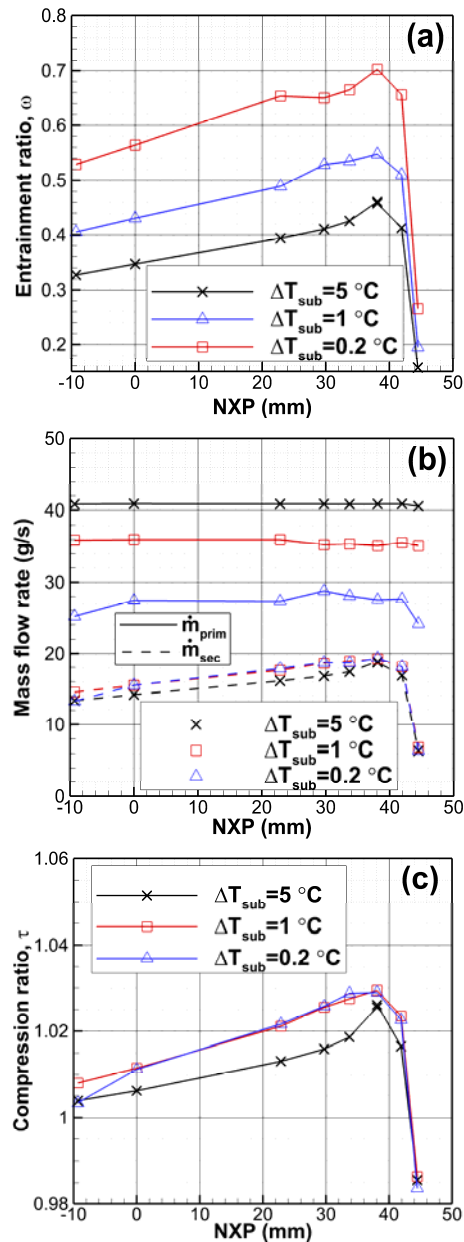


Fig. 7. Primary inlet subcooling and NXP: (a) entrainment ratio (b) mass flow rate (c) compression ratio.

A similar trend to that reported in Fig. 5 above is observed for the ejector behavior when the primary nozzle position is varied. A gradual improvement of the entrainment (Fig. 7a) and the compression (Fig. 7c) ratios is observed up to an optimal value of NXP, and then a sharp degradation of the performances follows. The optimal NXP value (38.1 mm) is the same as obtained previously, and this position is not sensitive to the variations of the subcooling imposed at the primary inlet. For the case with $\Delta T_{sub} = 0.2^\circ\text{C}$, a displacement of the primary nozzle from NXP = 10 mm to the optimal position, results in an improvement of the entrainment ratio about 32%. On the other hand, the improvement of the compression ratio is modest of

the order of 2%.

The variation of the subcooling imposed at the primary inlet has a large impact on the entrainment ratio (Fig. 7a). At NXP = 22.8 mm, the entrainment ratio increases about 66% when the subcooling level decreased from 5°C to 0.2°C . The mass flow rates observed in Fig. 7b show that this improvement of the entrainment ratio is mainly due to the decrease in primary flow rate ($\approx 33\%$), and to a slight progress of the secondary flow rate at the suction ($\approx 10.9\%$).

The variation of the compression ratio (Fig. 7c) with the subcooling is insignificant (less than 1%). However, the trend is consistent, since the decrease of the subcooling improves the entrainment ratio, thus the resulting flow mixture with a higher vapor content is expected to improve its overall compressibility.

3.2. Outlet Pressure and NXP

For various positions of the primary nozzle, the effects of the pressure at the outlet of the ejector on the entrainment ratio, the mass flow rates and the compression ratio of the ejector are shown in Fig. 8. The primary pressure was set at 14.9 bar, with a subcooling degree of 0.2°C . Three pressures at the ejector outlet were imposed: 3.7 bar, 4.2 bar and 4.7 bar.

As with the previous results, the trend of the ejector behavior with the displacement of the primary nozzle remains similar. The new curve with $P_{out} = 4.7$ bar also presents a peak value around NXP = 38.1 mm, and the optimal NXP is independent of the outlet pressures.

Between $P_{out} = 3.7$ bar and $P_{out} = 4.2$ bar, the entrainment ratio remains essentially unchanged, as Fig. 8a shows, due to the almost constant mass flow rates, represented in Fig. 8b. In this range of pressures, the flow rate turns out to be insensitive to downstream conditions. A further increase of the outlet pressure ($P_{out} = 4.7$ bar) results in a primary mass flow rate decrease and a slight decline of the secondary mass flow rate, consequently improving the entrainment ratio by about 8.5% at the optimal NXP position.

In terms of compression ratio, Fig. 8c shows that decreasing the pressure at the outlet of the ejector provides a slight improvement in compression, around 1.6% at optimal NXP. This gain in the compression ratio results mainly from a pressure decrease at the secondary stream inlet. Probably, with a lower pressure at the ejector outlet improves the expansion of the primary stream resulting in a lower pressure at the primary nozzle, which in turn is transmitted to the secondary inlet.

3.3. NXP and Pressure Inside Ejector

The impact of different nozzle positions on the pressure variation along the ejector are presented in Fig. 9. The pressure sensors installed at the ejector inlets and outlet as well as inside (see Fig. 3) made it possible to quantify the expansion of the

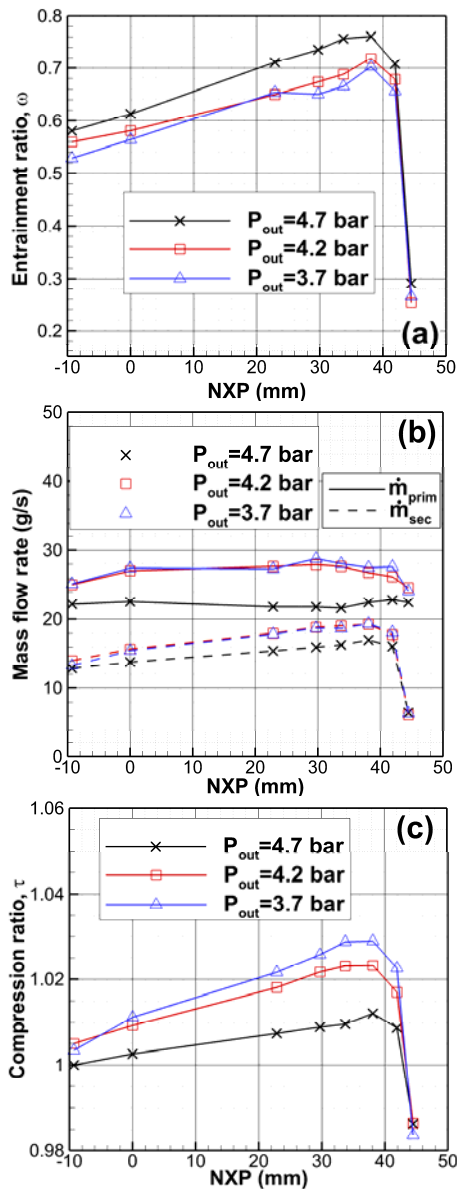


Fig. 8. Outlet pressure and NXP: (a) entrainment ratio (b) mass flow rate (c) compression ratio.

secondary flow, the compression of the mixture inside the constant section zone of the mixing chamber and the recompression in the diffuser. The experimental results in this respect were obtained by imposing the pressure at the ejector inlet and outlet respectively as 14.9 bar and 3.7 bar. A 0.2 °C degree of subcooling at the primary inlet was kept constant; this condition is close to saturation, as generally encountered in conventional refrigeration systems. To draw Fig. 9, previous NXP positions are represented, except the last one (NXP=44.48 mm), due to the significant uncertainty on pressure measurement. In fact, the proximity of the primary nozzle outlet with the pressure transmitter tapping is thought to be the main disturbance factor of the measurement discarded.

Moving the primary nozzle downstream increases the expansion of the secondary flow between the inlet and the mixing section (Fig. 9a). By advancing the primary nozzle into the mixing chamber, the

shape of the secondary nozzle changes such that the flow is accelerated, decreasing the pressure in the process. The entrainment ratio increases due to more important expansion at the secondary flow.

Figure 9 b shows that the primary nozzle displacement downstream improves the pressure rise in the mixing chamber zone with constant cross-section and in the diffuser. Indeed, between the two extreme NXP positions, the pressure rise is almost three times for the mixing section and about 45% for the diffuser. For $NXP \leq 0$, the constant-cross section zone of the mixing chamber experiences a pressure drop; by moving the nozzle forward the trend is reversed. The displacement of the nozzle possibly reinforces the conditions for the occurrence of weak condensation shocks in the mixing chamber and contributes to pressure rise in this zone.

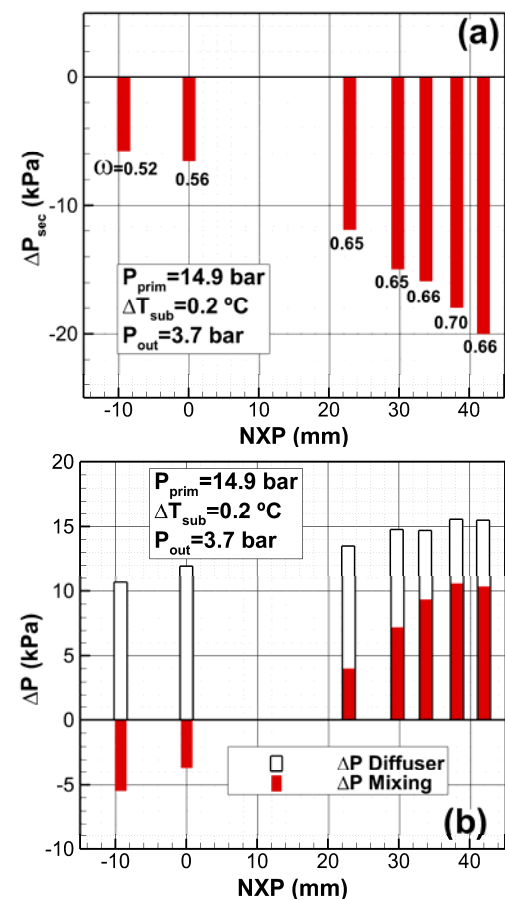


Fig. 9. NXP and pressure variation inside the ejector: (a) secondary flow expansion (b) compression in mixing chamber and diffuser.

4. CONCLUSION

Experimental data for R134a two-phase ejector were presented in the following context of operation: primary inlet pressure 8.8-14.9 bars, subcooling 0.2-5 °C and ejector outlet pressure 3.7-4.7 bars. Various thermodynamic states of the fluid at the inlet and outlet of the ejector, as well as the changes in internal geometry determined by the position of the primary nozzle relative to the mixing chamber were explored and their influence on

performance was assessed. The experimental data generated are important information for the design of refrigeration systems integrating a two-phase, liquid-vapour ejector.

The primary nozzle position and its displacement relatively to the mixing chamber affects performance, such that an optimal position in terms of ejectors characteristic performance parameters can be found. Beyond this position, ejector performance deteriorates rapidly. Improvements in the entrainment ratio can reach 32% while the compression ratio increase remains modest, approximately 2%. The optimal value of NXP was found to be 38.1 mm for the present tests; this position is not very sensitive to the variation of the conditions imposed at the ejector inlet-outlet.

Pressures at the ejector primary inlet and outlet have a limited impact on the entrainment ratio (less than 10% variation). On the other hand, the effect of primary flow subcooling is important, mainly due to the large variation in the mass flow rate. By varying the subcooling, from 5 °C to 0.2 °C, the entrainment ratio increases by nearly 66% at a certain nozzle position. The different operating conditions tested had little impact on the compression ratio (less than 2%).

Inside pressure monitoring showed a strong relation between NXP and pressure variations in the mixing section and the diffuser. Moving the nozzle forward improves the expansion of the secondary flow, and also the compression in the mixing section and the diffuser.

Future experimental tests, with the optimal NXP found, are expected with larger ranges of operating conditions.

ACKNOWLEDGEMENTS

This project was funded by PERD, a program of Natural Resources Canada for R-D.

REFERENCES

- Ameer, K., Z. Aidoun, M. Ouzzane (2016), Analysis of the Critical Conditions and the Effect of Slip in Two-Phase Ejectors, *J. Applied Fluid Mechanics* 9, Special Issue 2. 213–222.
- Ameer, K., Z. Aidoun, and M. Ouzzane (2017), Expansion of subcooled refrigerant in two-phase ejectors with no flux induction, *Exp. Therm. Fluid Sci.* 82, 424–432.
- Aphornratana, S. and I. W. Eames (1997), A small capacity steam-ejector refrigerator: experimental investigation of a system using ejector with movable primary nozzle, *Int. J. Refrig.* 20(5), 352–358.
- Banasiak, K., M. Palacz, A. Hafner, Z. Bulinski, J. Smolka, A. J. Nowak, A. Fic (2014), A CFD-based investigation of the energy performance of two-phase R744 ejectors to recover the expansion work in refrigeration systems: An irreversibility analysis, *Int. J. Refrig.* 40, 328–337.
- Chen, J., S. Jarall, H. Havtun, and B. Palm (2015). A review on versatile ejector applications in refrigeration systems, *Renew. Sustain. Energy Rev.* 49, 67–90.
- Chunnanond, K. and S. Aphornratana (2004), An experimental investigation of a steam ejector refrigerator: The analysis of the pressure profile along the ejector, *Appl. Therm. Eng.*, vol. 24, no. 2–3, pp. 311–322.
- Eames, I. W., A. E. Ablwaifa, and V. Petrenko (2007), Results of an experimental study of an advanced jet-pump refrigerator operating with R245fa, *Appl. Therm. Eng.*, vol. 27, no. 17–18, pp. 2833–2840.
- Hu, J., J. Shi, Y. Liang, Z. Yang, and J. Chen (2014), Numerical and experimental investigation on nozzle parameters for R410A ejector air conditioning system, *Int. J. Refrig.*, vol. 40, pp. 338–346.
- Huai, Y., X. Guo, and Y. Shi (2017), Experimental Study on Performance of Double-throttling Device Transcritical CO₂ Ejector Refrigeration System, *Energy Procedia*, vol. 105, pp. 5106–5113.
- Lin, C., W. Cai, Y. Li, J. Yan, Y. Hu, K. Giridharan (2013), Numerical investigation of geometry parameters for pressure recovery of an adjustable ejector in multi-evaporator refrigeration system, *Appl. Therm. Eng.* Vol. 61, pp. 649-656.
- Liu, F., Y. Li, E. A. Groll, (2012), Performance enhancement of CO₂ air conditioner with a controllable ejector, *Int. J. Refrig.*, vol. 35 pp. 1604–1616.
- Palacz, M., J. Smolka, A.J. Nowak, K. Banasiak, A. Hafner (2017), Shape optimisation of a two-phase ejector for CO₂ refrigeration systems, *Int. J. Refrig.*, vol. 74, pp. 212–223.
- Ren, L. Q., X. M. Guo, X. W. Guo, and T. L. Li (2014), Experimental Study on Performance of Two-phase Ejector Refrigeration Cycle System with Two-throat Nozzle. In *Proceedings of International Refrigeration and Air Conditioning Conference, paper 1472*, Purdue.
- Varga, S., A. C. Oliveira, and B. Diaconu (2009), Influence of geometrical factors on steam ejector performance - A numerical assessment, *Int. J. Refrig.* 32 (7). 1694–1701.
- Wang, X. and J. Yu (2016), Experimental investigation on two-phase driven ejector performance in a novel ejector enhanced refrigeration system, *Energy Convers. Manag.*, 111, 391–400.
- Yazdani, M., A. Alahyari, T. Radcliff (2012), Numerical modeling of two-phase supersonic ejectors for work-recovery applications, *Int. J. Heat Mass Transf.* 55, 5744–5753.
- Zhu, Y., W. Cai, C. Wen, and Y. Li, (2009), Numerical investigation of geometry parameters for design of high performance ejectors, *Appl. Therm. Eng.*, 29 (5–6), 898–905.

